



MIT Open Access Articles

Human hepatocellular carcinoma diagnosis by multiphoton autofluorescence microscopy

The MIT Faculty has made this article openly available. **Please share** how this access benefits you. Your story matters.

Citation	Sun, Tzu-Lin et al. "Human hepatocellular carcinoma diagnosis by multiphoton autofluorescence microscopy." Advanced Biomedical and Clinical Diagnostic Systems VIII. Ed. Tuan Vo-Dinh, Warren S. Grundfest, & Anita Mahadevan-Jansen. San Francisco, California, USA: SPIE, 2010. 75551L-9. ©2010 SPIE.
As Published	http://dx.doi.org/10.1117/12.843157
Publisher	SPIE
Version	Final published version
Accessed	Wed Dec 05 12:20:18 EST 2018
Citable Link	http://hdl.handle.net/1721.1/58568
Terms of Use	Article is made available in accordance with the publisher's policy and may be subject to US copyright law. Please refer to the publisher's site for terms of use.
Detailed Terms	

Human Hepatocellular Carcinoma Diagnosis by Multiphoton Autofluorescence Microscopy

Tzu-Lin Sun^{1#}, Yuan Liu^{1#}, Ming-Chin Sung¹, Hsiao-Ching Chen², Chuen-Huei Yang¹, Vladimir Hovhannisyanyan¹, Ling-Ling Chiou², Wei-Chou Lin³, Guan-Tarn Huang², Ki-Hean Kim⁴, Peter T. C. So⁴, Chih-Ju Lin¹, Hsuan-Shu Lee^{2&}, Chen-Yuan Dong^{1*}

¹*Department of Physics, National Taiwan University, Taipei 106, Taiwan*

²*Department of Internal Medicine, National Taiwan University Hospital and National Taiwan University, College of Medicine, Taipei 100, Taiwan*

³*Department of Pathology, National Taiwan University Hospital and National Taiwan University, College of Medicine, Taipei 100, Taiwan*

⁴*Department of Mechanical Engineering and the Division of Bioengineering, Massachusetts Institute of Technology, MA, Cambridge 02139*

[#]These authors contributed equally to this work.

Address all correspondence to [&]Hsuan-Shu Lee, National Taiwan University, Taipei 106, Taiwan; Tel: +886-2-3366-6007; Fax: +886-2-3366-6001; E-mail: benlee@ha.mc.ntu.edu.tw or *Chen-Yuan Dong, Department of Physics, National Taiwan Univ., Department of Physics National Taiwan University, Taipei, Taiwan 106 Taiwan; Tel: +886-2-3366-5155; Fax: +886-2-2363-9984; E-mail: cydong@phys.ntu.edu.tw

Abstract

We apply multiphoton microscopy for the qualitative imaging and quantitative analysis of hepatocellular carcinoma (HCC) of different grades under *ex-vivo*, label-free conditions, and found that multiphoton autofluorescence (MAF) is effective in identifying cellular architecture in the liver specimens, and can be used to obtain quantitative parameters for characterizing the disease. Our results demonstrates the capability of using tissue quantitative parameters of multiphoton autofluorescence (MAF), the nuclear number density (NND), and nuclear-cytoplasmic ratio (NCR) for tumor discrimination, and the potential of this technique in clinical diagnosis of HCC and in *in-vivo* investigation of liver tumor development of animal models.

Keywords: hepatocellular carcinoma, multiphoton, autofluorescence

Introduction

In recent years, considerable interests have been placed on the use of minimally-invasive, optical imaging techniques for disease diagnosis. Among the various imaging modalities, diffusive imaging allows the deepest imaging depths at mm resolution to be achieved.^(1, 2) In comparison, interferometric technique such as optical coherent tomography (OCT) can provide tissue morphological information to depths in the mm range and resolution approaching the μm scale.^(3, 4) The highest resolution is provided by confocal microscopy which is capable of imaging subcellular organelles. However, due to the absorption and scattering of the visible excitation photons used for imaging, the penetration depth of confocal microscopy is limited to the 100 μm range.⁽⁵⁻⁷⁾ As an alternative imaging modality, multiphoton microscopy, in recent years, has emerged to be a promising technique for the qualitative and quantitative characterization of pathological tissues. Specifically, the high axial-depth discrimination capability, reduced photodamage, and enhanced penetration depths render this technique as the preferred tool for minimally-invasive diagnosis in the clinics.⁽⁸⁻¹²⁾ Moreover, non-linear polarization effects such as second harmonic generation (SHG) may be used to characterize the extent of abnormal growth of the extracellular matrix such as collagen fibrosis. Previous studies have demonstrated the effectiveness of multiphoton imaging in diagnosing pathological tissues such as skin aging, basal cell carcinoma, atherosclerosis, corneal keratitis, keratoconus, and optical nerve head abnormalities.⁽¹³⁻¹⁹⁾

Hepatology, as in many other areas of biology and medicine, relies heavily on histopathological examination for disease diagnosis. In serious diseases such as hepatocellular carcinoma (HCC) and liver fibrosis, diagnosis is performed by qualitative examination of histopathological specimens. In the case of HCC, a qualitative grading system⁽¹⁻⁴⁾ has been developed and is in common usage.^(20, 21) However, the inability to follow subsequent tissue dynamics and concerns over specimen preparation artifacts limits the application of histological methods in research. In addition, one often needs to consider potential artifacts associated with histological preparation. Finally, the lack of quantitative parameters can make histological examination unreliable. In this study, we attempt to address some of these issues by performing *ex-vivo* imaging and quantitative analysis of HCC. Without extrinsic labeling, we attempt to demonstrate that the multiphoton signatures from the tissue specimens can provide useful qualitative and quantitative indications of the diseases' progressions. Specifically, quantitative parameters such as nuclear number density (NND), nucleus to cytoplasm ratio (NCR), and multiphoton autofluorescence intensity ratio (MAFIR) between tumor (T) and non-tumor (NT) tissues are used.

Materials and Methods

Multiphoton Imaging System

The multiphoton imaging system used in this study is similar to one previously described.¹³ We used the 780 nm, 80 MHz output of a femtosecond, titanium-sapphire laser (Tsunami, Spectra Physics, Mountain View, CA) pumped by a diode-pumped solid-state laser (Millennia X, Spectra Physics) for specimen excitation. The excitation light was guided into a modified upright microscope (E800, Nikon, Japan), and expanded to overfill the objective's back aperture. The expanded beam is reflected into the high numerical aperture focusing objective (S Fluor 40X/NA 1.3

Oil, Nikon) by a dichroic mirror (435DCXR, Chroma Technology, Rockingham, VT). The MAF and SHG produced at the focal spot is collected in the epi-illuminated geometry and separated by a secondary dichroic and additional band pass filters (E435LP 700SP, HQ 390/20, Chroma Technology) for the respective collection and isolation of broadband autofluorescence (MAF, 435-700 nm) and SHG (380-400 nm) signals. Single-photon counting photomultiplier tubes (R7400P, Hamamatsu, Japan) and the respective discriminators were used for the detection and processing of the signal photons. The signal photons were processed using the single-photon counting mode.

Preparation of Frozen and Paraffin Fixation Specimens

In this study, two adjacent tissue blocks from the resected liver of each patient were used. One specimen was frozen while the other specimen underwent traditional histological preparation procedures. The histological specimens of T and the corresponding NT tissue specimens from the same HCC patient were fixed in 10% formalin followed by conventional paraffin fixation procedure, and labeled with hematoxylin and eosin (H&E) dyes. In our study, the H&E specimens are used for histopathological diagnosis and comparison with the multiphoton imaging results.

To eliminate the effects of chemical species such as H&E dyes or paraffin on the detected MAF and SHG, we elected to use frozen specimens for multiphoton imaging applications. From each tissue block we made 25 frozen fixation specimens of 25 adjacent sections. Each frozen specimen was embedded in optimal cutting temperature (O.C.T.) compound. Prior to performing multiphoton imaging, the frozen specimens were covered with aluminum foils and frozen at -80°C .

Image Calibration and Correction

For image calibration, a uniform 0.05 mg/ml rhodamine 110 (Molecular Probes, Eugene, OR) specimen was used. Before each experiment, the multiphoton microscope is calibrated by measuring the fluorescence intensity of the rhodamine 110 solution (0.05 mg/ml). The specimen is imaged from the surface at different depths to identify the position of maximum fluorescence intensity. At the depth of maximum fluorescence, 25 images were obtained and the fluorescence intensities of the images are averaged and used for intensity calibration. In addition, since the multiphoton signal profiles along the x and y axes are well approximated by a parabola, multiphoton images of the T and NT specimens shown in the Results section were corrected using a custom program for correcting intensity heterogeneity of the image field.⁽²²⁾

Quantitative Analysis of HCC

In addition to performing multiphoton imaging of the liver specimens, we also analyzed the NND, NCR, and the MAFIR between the T and NT tissues from the images in order to establish a quantitative link differentiating T from NT tissues.

HCC Nuclear Number Density (NND) Analysis

As a demonstration of our NND analysis approach, we determined the nuclei number within an image area $330 \times 220 \mu\text{m}^2$ in size of an NT specimen (Fig. 1). The raw multiphoton image is shown in Fig. 1(a). Since nuclei lack MAF (yellow arrows), the raw multiphoton image is inverted for a clear identification of the individual nuclei (Fig. 1(b), red arrows). The ImageJ software (NIH) was then used to mark the nuclear positions (Fig.1 (c)) for the automatic determination of the nuclear number (Fig.1 (d)).

HCC Nucleus to Cytoplasm Ratio (NCR) Analysis

A second metric we used to differentiate the T and NT tissue specimens is the NCR. To demonstrate our approach in the NCR analysis, the same $330 \times 220 \mu\text{m}^2$ area in Fig. 1 was used for analysis. In imaging the liver tissue specimens, we found that the MAF intensity of the nuclear region is much lower than that of the cytoplasm. For NCR determination, we randomly selected 5 nuclei and determined their average MAF intensity. The measured value was then used as the threshold parameter for discriminating the nuclei from the cytoplasmic domains. The total pixel numbers below the MAF intensity threshold represents the total area occupied by the nuclear regions in the image. The cytoplasmic area is then determined by subtracting the nuclear area from the total image area. The NCR can then be obtained from the ratio of the area occupied by the nuclear region over that of the cytoplasmic domain.

HCC Autofluorescence (MAFIR) Analysis

In addition to performing the NND and NCR analysis, we also determined the average MAF intensity of the imaged area ($1100 \times 1100 \mu\text{m}^2$ in size). Results for both the T and NT regions of each patient were determined, and MAFIRs of the T to NT regions were computed.

Results

Shown in Figs. 2 (a) is the MAF images of HCC grade 1. For comparison, histological images (Fig. 2(b)) of H&E prepared tissue samples are shown. Since frozen specimens were used for multiphoton imaging and H&E labeled tissues used for histological examinations, the multiphoton images and their histological comparison are from different tissue blocks of the same patient. The multiphoton images shown in Fig. 2 demonstrate the effectiveness our approach in imaging and distinguishing the nuclei HCC tissues.

As the enlarged images show (Fig. 2 (c), (d)), since cellular nuclei lack MAF, individual hepatocytes can be identified by non-autofluorescent round domains surrounded by autofluorescent cytoplasm (yellow arrows). On the other hand, the presence of fibrous collagen fibers can be identified by the spectrally distinct SHG signal (white arrows).

Although qualitative multiphoton imaging can provide us with label-free, structural information of the hepatocytes in the HCC specimens, additional diagnostic parameters can be derived from quantitative analysis of the multiphoton images.

Nuclear number density (NND) analysis

One parameter we derived from quantitative image analysis is the nuclear number density (NND). Numerical results of NND analysis are plotted in Fig. 3. Fig. 3(a) is our result of the nuclear number per $100 \times 100 \mu\text{m}^2$ area for different and for all grades of imaged liver tissue. Fig. 3 (a) shows, the nuclear number density among the individual T and NT groups do not vary much. However, for each HCC grade, the NND of T specimens is significantly higher than that of the NT specimens. In Fig. 3 (a), we also plot the NND ratios for T and NT specimens for all tissues imaged, and we found that the overall NND values of T and NT tissue specimens are 36.51 ± 8.81 and 17.07 ± 3.04 respectively, with the T value being 2.14 times higher than that of the NT result. Our result shows that the NND ratio obtained from label-free multiphoton imaging is an effective quantitative parameter for discriminating the T and NT specimens.

Nucleus to Cytoplasm (NCR) analysis

Another parameter we quantified and used for discriminating T from the NT tissues is the nuclear-cytoplasmic ratio (NCR). Results of Fig.3 (b) show that for each HCC grade, the NCR's of the T specimens are higher than that of the NT specimens. In Fig. 3(b), the NCR's for both all T and NT specimens are also combined and displayed. We found that the overall NCR for T specimens is 4.94 times that of the NT specimens. From our result, one sees that the NCR derived from label-free multiphoton imaging and quantitative analysis is an effective parameter can be used for discriminating T and NT liver tissues.

Autofluorescence Intensity Ratio (MAFIR) Analysis

The final metric we used to for the quantitative classification and discrimination of HCC is the MAF intensity. To avoid patient to patient sample variation, we analyze the MAFIR of the T to NT tissue for each patient. The results shown in Fig. 3(c) indicate that the MAFIR for T to NT tissue is less than one for each HCC grade, implying the MAF intensity of the T region is less than that of the NT area. This result demonstrates that by comparing the MAF intensity of different sections of liver tissue from the patient can be used to quantitatively discriminate the T from the NT regions.

Discussion

The current classification of HCC is performed by the qualitative examination of biopsied liver tissue specimens, and HCC diagnosis largely based on the morphologic differences between the tumor and normal tissues. However, the lack of quantitative analysis can add uncertainty in the diagnostic process. Furthermore, histological examination procedures prevent *in-vivo* disease diagnostics and investigation of physiological processes to be performed. In this work, we attempted to classify and distinguish HCC tissues by both qualitative, label-free imaging and quantitative image analysis. We found that MAF and SHG imaging allow the respective identification of individual hepatocytes and collagen fibers in the HCC specimens, and the quantitative parameters of nuclear number density (NND), the nuclear-cytoplasmic ratio (NCR), and autofluorescence (AF) intensity ratio (MAFIR) enables clear discrimination of T from NT tissues. These findings are particularly important in early stages of HCC as the proliferation of cancer cells is not apparent and the appearance of the nuclei is almost uniform. The difficulties in discriminating early, grade 1 HCC tissues by morphological examination need to be addressed by additional biochemical analysis. This issue can be circumvented by multiphoton imaging as we found that the MAF intensity of NT tissues is significantly higher than that of the T tissue. From our result, the analysis of MAFIR between T and NT tissues can be used to assist the discrimination of HCC grade1 in a definitive fashion. In addition, we find that the overall NND of T tissue is 2.14 times that of NT tissue, and that the NCR of T tissue is 4.94 times that of NT tissue. These three parameters can be applied to quantitatively diagnose HCC, and assist physicians in the diagnostic process. In combination with intravital imaging technologies of the liver,⁽²³⁾ our approach can be extended to *in-vivo* models to aid the investigation of the physiological mechanics of HCC formation, or the immune reaction in the disease. These efforts can contribute to a better understanding of liver malignancy and develop more effective treatment procedures.

Figure and Figure Captions

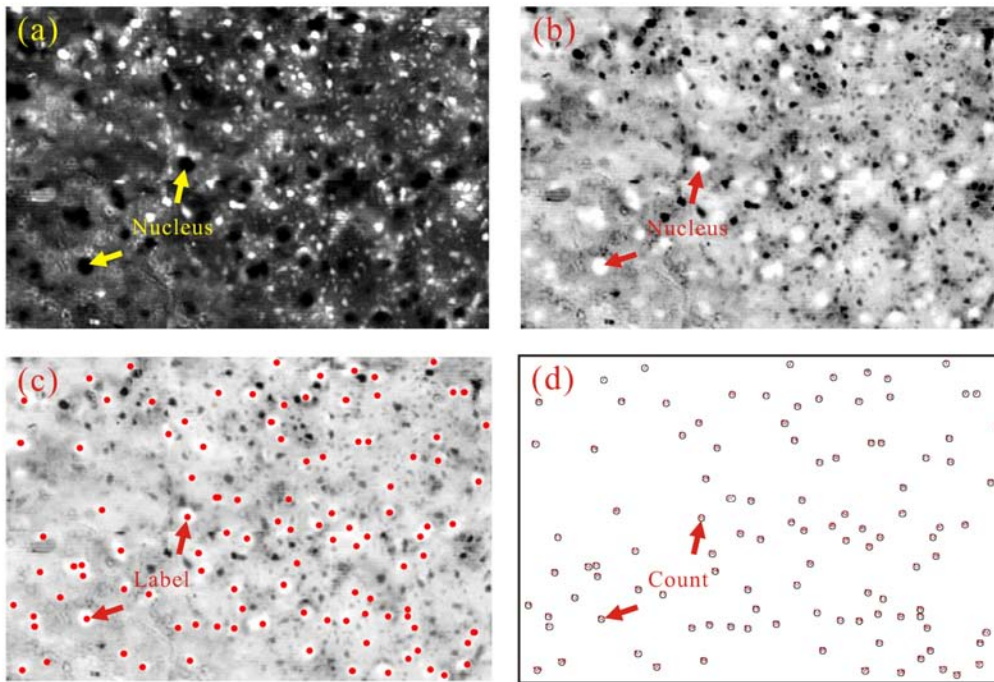


Fig. 1 a) MAF images of NT specimens. Individual dark regions (MAF lacking) are the cell nuclei (yellow arrows). b) Tissue image after MAF intensity inversion. The bright nuclei (red arrows) can be used for cellular identification. c) Automatic counting of the nuclei (red spots) using the ImageJ software. d) These circular domains correspond to the nuclei positions. The nuclear number of 107 within the $330 \times 220 \mu\text{m}^2$ image corresponds to a nuclear number density of 14.74 per $100 \times 100 \mu\text{m}^2$ area. The nuclear number density of both NT and T specimens can be determined using this approach.

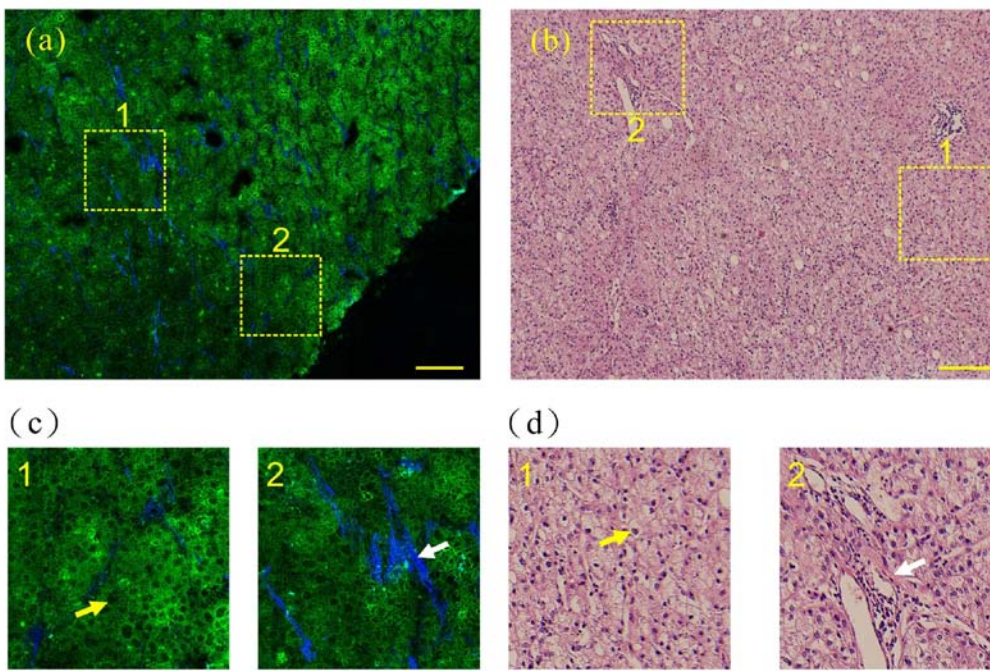


Fig. 2 (a) Large-area multiphoton imaging of a grade 1 HCC specimen. (b) Histological comparison and (c) magnified multiphoton images of selected regions of interest of (a). (d) Comparative histological images show that hepatocyte nuclei can be identified by their lack of autofluorescence (yellow arrows) and fibrotic collagen can be traced using SHG imaging (white arrows). Green: MAF, blue: SHG. Scale bar is 200 μm .

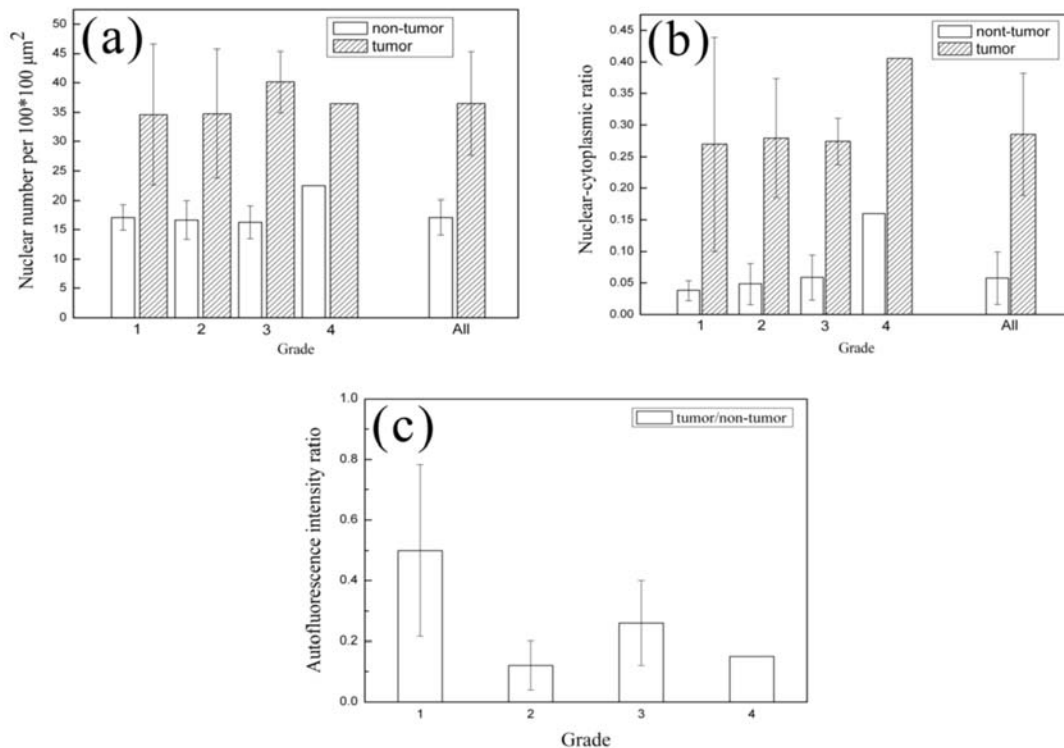


Fig. 3 a) NND predetermined for an area of $100 \times 100 \mu\text{m}^2$ for T and NT tissues. The number of specimens corresponding to grades 1 to 4 HCC is 3, 4, 5, and 1 respectively. b) NCR analysis of differently graded T and NT tissues. The specimen numbers corresponding to grades 1 to 4 are 3, 4, 5, and 1 respectively. c) MAFIR analysis between T and NT tissues shows that for each HCC grade, the MAFIR of T is lower than that of NT. The specimen numbers corresponding to grade 1 to 4 HCC are respectively 4, 7, 10, and 1.

References

1. Q. Zhu, E. Conant and B. Chance, "Optical imaging as an adjunct to sonograph in differentiating benign from malignant breast lesions," *J Biomed Opt* 5(2), 229-236 (2000)
2. K. Tanner, E. D'Amico, A. Kaczmarowski, S. Kukreti, J. Malpeli, W. W. Mantulin and E. Gratton, "Spectrally resolved neurophotonic: a case report of hemodynamics and vascular components in the mammalian brain," *J Biomed Opt* 10(6), - (2005)
3. D. Huang, E. A. Swanson, C. P. Lin, J. S. Schuman, W. G. Stinson, W. Chang, M. R. Hee, T. Flotte, K. Gregory, C. A. Puliafito and J. G. Fujimoto, "Optical Coherence Tomography," *Science* 254(5035), 1178-1181 (1991)
4. G. J. Tearney, M. E. Brezinski, B. E. Bouma, S. A. Boppart, C. Pitris, J. F. Southern and J. G. Fujimoto, "In vivo endoscopic optical biopsy with optical coherence tomography," *Science* 276(5321), 2037-2039 (1997)
5. M. Rajadhyaksha, M. Grossman, D. Esterowitz and R. H. Webb, "In-Vivo Confocal Scanning Laser Microscopy of Human

Skin - Melanin Provides Strong Contrast," *Journal of Investigative Dermatology* 104(6), 946-952 (1995)

6. M. Rajadhyaksha, M. Grossman, R. H. Webb and R. R. Anderson, "Video-Rate Confocal Scanning Laser Microscopy of Live Human Skin," *Journal of Investigative Dermatology* 104(4), 618-618 (1995)
7. B. R. Masters and M. Bohnke, "Three-dimensional confocal microscopy of the living human eye," *Annual Review of Biomedical Engineering* 4(69-91) (2002)
8. W. Denk, J. H. Strickler and W. W. Webb, "2-Photon Laser Scanning Fluorescence Microscopy," *Science* 248(4951), 73-76 (1990)
9. P. T. C. So, C. Y. Dong, B. R. Masters and K. M. Berland, "Two-photon excitation fluorescence microscopy," *Annual Review of Biomedical Engineering* 2(399-429) (2000)
10. A. Zoumi, A. Yeh and B. J. Tromberg, "Imaging cells and extracellular matrix in vivo by using second-harmonic generation and two-photon excited fluorescence," *Proceedings of the National Academy of Sciences of the United States of America* 99(17), 11014-11019 (2002)
11. W. R. Zipfel, R. M. Williams and W. W. Webb, "Nonlinear magic: multiphoton microscopy in the biosciences," *Nature Biotechnology* 21(11), 1368-1376 (2003)
12. P. J. Campagnola and L. M. Loew, "Second-harmonic imaging microscopy for visualizing biomolecular arrays in cells, tissues and organisms," *Nature Biotechnology* 21(11), 1356-1360 (2003)
13. S. J. Lin, R. J. Wu, H. Y. Tan, W. Lo, W. C. Lin, T. H. Young, C. J. Hsu, J. S. Chen, S. H. Jee and C. Y. Dong, "Evaluating cutaneous photoaging by use of multiphoton fluorescence and second-harmonic generation microscopy," *Optics Letters* 30(17), 2275-2277 (2005)
14. S. J. Lin, S. H. Jee, C. J. Kuo, R. J. Wu, W. C. Lin, J. S. Chen, Y. H. Liao, C. J. Hsu, T. F. Tsai, Y. F. Chen and C. Y. Dong, "Discrimination of basal cell carcinoma from normal dermal stroma by quantitative multiphoton imaging," *Optics Letters* 31(18), 2756-2758 (2006)
15. R. Cicchi, D. Massi, S. Sestini, P. Carli, V. De Giorgi, T. Lotti and F. S. Pavone, "Multidimensional non-linear laser imaging of Basal Cell Carcinoma," *Opt Express* 15(16), 10135-10148 (2007)
16. T. T. Le, I. M. Langohr, M. J. Locker, M. Sturek and J. X. Cheng, "Label-free molecular imaging of atherosclerotic lesions using multimodal nonlinear optical microscopy," *Journal of Biomedical Optics* 12(5), - (2007)
17. H. Y. Tan, Y. Sun, W. Lo, S. J. Lin, C. H. Hsiao, Y. F. Chen, S. C. M. Huang, W. C. Lin, S. H. Jee, H. S. Yu and C. Y. Dong, "Multiphoton fluorescence and second harmonic generation imaging of the structural alterations in keratoconus ex vivo," *Investigative Ophthalmology & Visual Science* 47(12), 5251-5259 (2006)
18. H. Y. Tan, Y. Sun, W. Lo, S. W. Teng, R. J. Wu, S. H. Jee, W. C. Lin, C. H. Hsiao, H. C. Lin, Y. F. Chen, D. H. K. Ma, S. C. M. Huang, S. J. Lin and C. Y. Dong, "Multiphoton fluorescence and second harmonic generation microscopy for imaging infectious keratitis," *J Biomed Opt* 12(2), - (2007)
19. D. J. Brown, N. Morishige, A. Neekhra, D. S. Minckler and J. V. Jester, "Application of second harmonic imaging microscopy to assess structural changes in optic nerve head structure ex vivo," *J Biomed Opt* 12(2), - (2007)
20. H. A. Edmondson and P. E. Steiner, "Primary Carcinoma of the Liver - a Study of 100 Cases among 48,900 Necropsies," *Cancer* 7(3), 462-503 (1954)
21. Z. Schaff and P. Nagy, "Pathology Techniques and Grading Systems in the Diagnosis of HCC," in *Liver cancer* K. Okuda

and E. Tabor, Eds., pp. 111-113, Churchill Livingstone, New York (1997).

22. V. A. Hovhannisyan, P. J. Su, Y. F. Chen and C. Y. Dong, "Image heterogeneity correction in large-area, three-dimensional multiphoton microscopy," *Optics Express* 16(7), 5107-5117 (2008)

23. Y. Liu, H. C. Chen, S. M. Yang, T. L. Sun, W. Lo, L. L. Chiou, G. T. Huang, C. Y. Dong and H. S. Lee, "Visualization of hepatobiliary excretory function by intravital multiphoton microscopy," *J Biomed Opt* 12(1), - (2007)